Morphodynamic equilibrium of alternate bar dynamics under repeated hydrographs

Dai Huang,¹ Qiujun Xie,¹ and Toshiki Iwasaki ²

- ¹ Changjiang Institute of Survey, Planning, Design and Research Corporation, 430010 Wuhan, China; e-mail: daihuangdd@outlook.com; Corresponding author.
- ² Faculty of Engineering, Hokkaido University, 0608628 Sapporo, Japan; e-mail: tiwasaki@eng.hokudai.ac.jp

ABSTRACT

Discharge unsteadiness plays a key role in the dynamics of alternate bars, however, how migrating alternate bars determine their shape under unsteady discharge conditions, especially in the long-term, is still unclear. In this study, we numerically investigate long-term behaviors of migrating alternate bars subject to repeated hydrographs. For this, the same discharge variation but different hydrograph cycles were tested. The results show that even under unsteady flow conditions, specific combinations of hydrograph cycles and discharge variations result in an equilibrium state of migrating alternate bars (i.e., non-time dependent wavelength and migration period). This may be a unique feature of the alternate bar morphodynamics, since dynamic equilibrium state arising from steady discharge counterparts is time-dependent feature.

Keywords: alternate bars, unsteady discharge, morphodynamic equilibrium

1. Introduction

The discharge unsteadiness is essential in river system and plays a critical role in the sand bar formation and dynamics that has not been achieved under steady discharge condition. Tubino performed a linear stability analysis of free river bars under unsteady discharge conditions to understand unsteady behaviors of alternate bar dynamics regarding weavelength and waveheight shown in the experimental flume. This first theoretical attempt indicated the importance of flow unsteadiness to bar dynamics and further motivated the understanding of alternate bar dynamics under unsteady discharge conditions. Visconti et al. conducted movable bed and bank experiments under unsteady discharge conditions, showing that a specific combination of hydrograph features and migration characteristics of bars enhance or suppress the development of pseudo-meandering channels. Iwasaki et al. performed a numerical simulation of the bar and bank erosion in the vegetated floodplain during a large flood in a natural river (Otofuke River, Japan), suggesting

similar importance of the discharge unsteadiness to the amplification of meandering channels.

This study focuses on the long-term behaviors of alternate bars under the influence of repeated hydrographs. The questions we pursue in this study are 1) Do alternate bars attain the equilibrium state under unsteady flow discharge conditions? 2) What are the equilibrium characteristics of alternate bars under this condition? To understand these points, we perform several numerical simulations of alternate bar formations under repeated hydrographs and corresponding steady discharge conditions using a two-dimensional morphodynamic model, iRIC-Nays2DH. The simulated alternate bar morphodynamics, i.e., the wavelength, bar height, and migration period, are investigated to understand the effect of hydrographs on long-term alternate bar characteristics, and the relation between hydrograph and morphodynamic timescales.

2. Method

2.1. Numerical model

We used the Nays2DH model, a two-dimensional morphodynamic model embedded in the iRIC software. This model was applied to various sediment transport-related simulation studies, and is suitable for simulating alternate bar morphodynamics focused on in this study. These model validations suggest that the Nays2DH model may be an acceptable tool to pursue the long-term morphodynamics of alternate bars under repeated hydrographs focused on in this study. Meanwhile, the flow model used is an unsteady two-dimensional shallow water flow model. As we focus on the morphodynamics of alternate bars in gravel-bed rivers, we only consider bedload transport as a mode of sediment transport. The Meyer-Peter and Müller formula was used here, and the sediment was assumed to have a uniform grain size.

2.2 Computational conditions

To understand the morphodynamics of alternate bars under repeated hydrographs, we used the condition of the Otofuke River as an example. This river is a typical gravel-bed river and the alternate bars are one of the dominant river morphologies. The modeled channel has a 21 km length and 70 m constant channel width with a uniform slope of 0.005. A Manning roughness coefficient of 0.028 s/m^{1/3} and a uniform particle size of 40 mm were used. The mesh size used in this study is 70 m×10 m, which means 7 grid sizes in width and 3000 sizes in length. The time step used in this study is 0.2 second. The initial bed is uniformly flat for transverse direction without any perturbation, but, random perturbation is added to the transverse profile of upstream discharge to obtain a trigger for alternate bar formation and development in entire calculation time.

We derived the hydrograph shape based on the large flood event observed in 2011, such that the migrating alternate bars could form and develop. This is a relatively large flood event of which the flood recurrence year is around 20 years and caused significant bar migration and subsequent amplification of the channel. The details can be found in previous works (e.g.,). Figures 1(a) and (b) show the observed hydrograph and simplified repeated hydrographs used in the calculation. The observed hydrograph was modeled as a simple triangle-shaped hydrograph; the water discharge linearly increased from 100 to 600 m³/s within 20 h and subsequently decreased from 600 to 100 m³/s linearly in 20 h, forming a 40 h cycle.

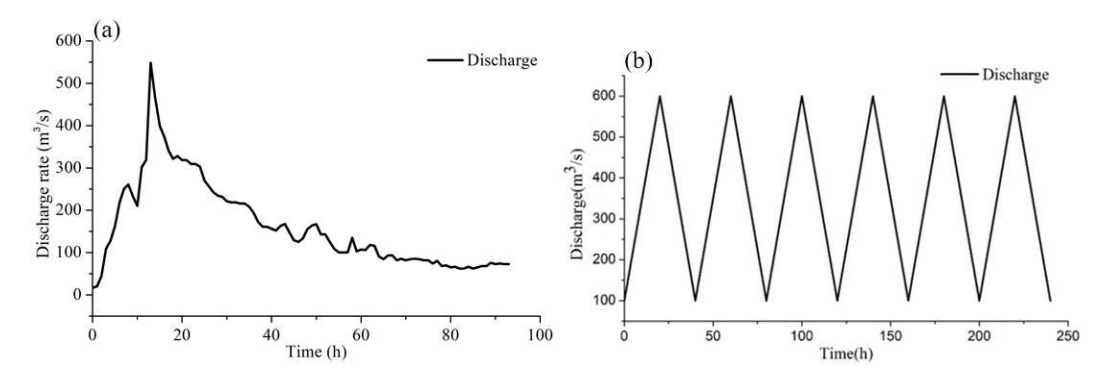


Figure 1 (a) Observed hydrograph of the 2011 flood in the Otofuke River, and (b) Hydrograph condition used for the calculation.

The six hydrographs are shown here as an example. In the calculation, 50 hydrographs were obtained. The aforementioned computational condition is the same as our previous studies that focus on the effect of sediment supply on the alternate bar formation. In the previous study, we have showed that imbalance of sediment supply from the upstream end under such hydrograph hardly affect the downstream alternate bars formation under this computational condition at least for timescale of single flood event. In this study, the sediment feed rate used was calculated from the upstream end flow parameters, just as same as one of the sediment conditions in our previous study. This feed rate is the sediment transport capacity of this modeled river, and the supply rate depends on the hydrograph, as shown in Figure 1(b). As the feed rate is equivalent to the transport capacity, the bed elevation at the upstream end does not change over time under this condition.

3. Results

3.1 Features of morphodynamic equilibrium state of alternate bars under repeated hydrographs

Figure 2 shows the elevation variation at the right bank of the computational river with respect to time. In this figure, the migration of alternate bars can be inferred from the pattern of elevation variation, that is, erosional and depositional patterns of this figure move from bottom-left to top-right. This pattern shows that the morphology (i.e., alternate bars) keeps migrating downstream, and the slope of this pattern shows the migration velocity of bars, as this figure represents the bed elevation contour of the time-space domain. It can be shown that although the

migration velocity varies owing to the unsteady water discharge, the average migration velocity of the alternate bars, which is akin to long-term behavior, appears constant. Additionally, the spacing between each depositional or erosional point, which corresponds to the wavelength of alternate bars, is consistent with respect to space and time. Figure 5 shows the temporal change of alternate bars during the last hydrograph of this computation. Here five typical time points in one hydrograph cycle are selected to present the characteristics of the alternate bars during a hydrograph. The points are 0 (beginning of the hydrograph cycle), 1/4T (one-quarter of the hydrograph cycle), 1/2T, 3/4T, and T (end of the hydrograph cycle), where T denotes the hydrograph cycle. As shown by the red arrow line, the migration velocity changes with respect to discharge, while the wavelength remains constant at 580 m with respect to time. Moreover, when t = 0 and t = T, the positions and shapes of alternate bars are identical; thus, the elevation of the river bed returns to its original value after one hydrograph cycle because alternate bars migrate exactly one wavelength downstream within one hydrograph.

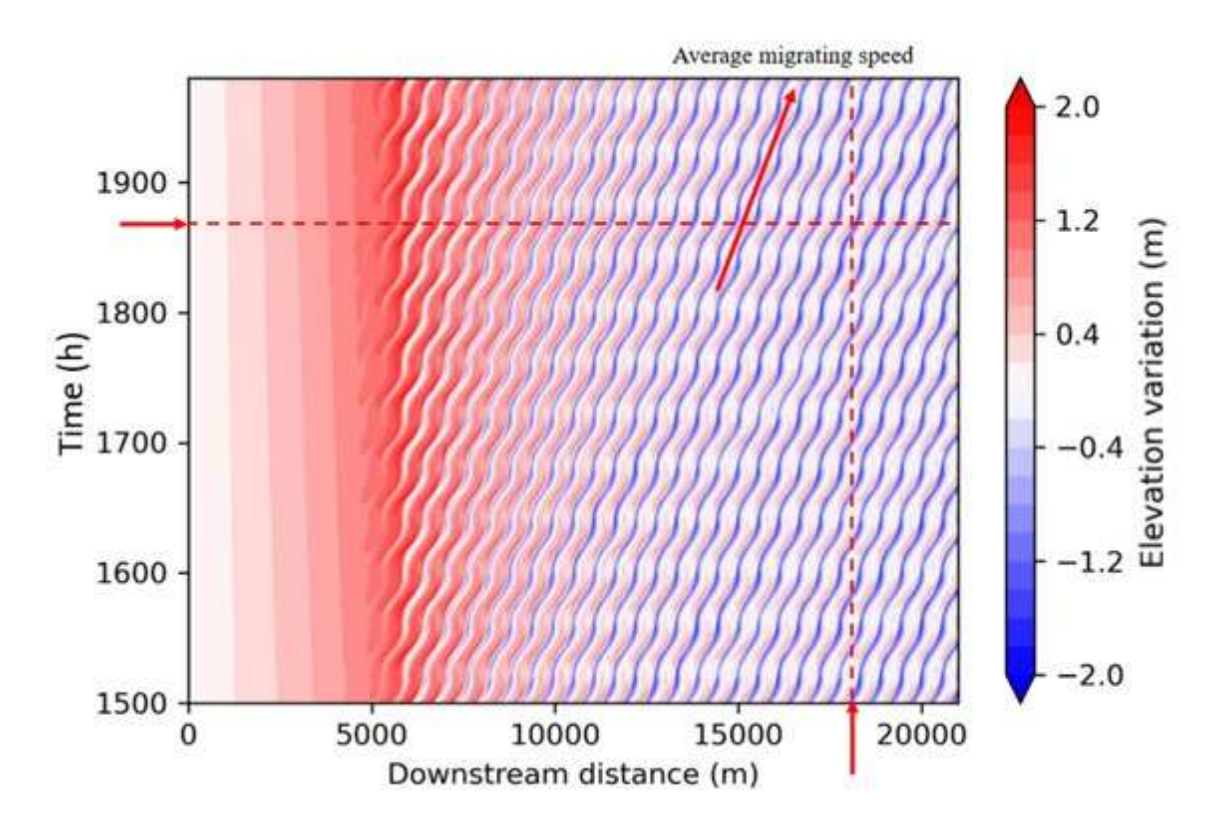


Figure 2 (Color) Elevation variation at the right bank along time and downstream distance. (The red dashes represent the elevation variation with time or distance in Figure 6 below)

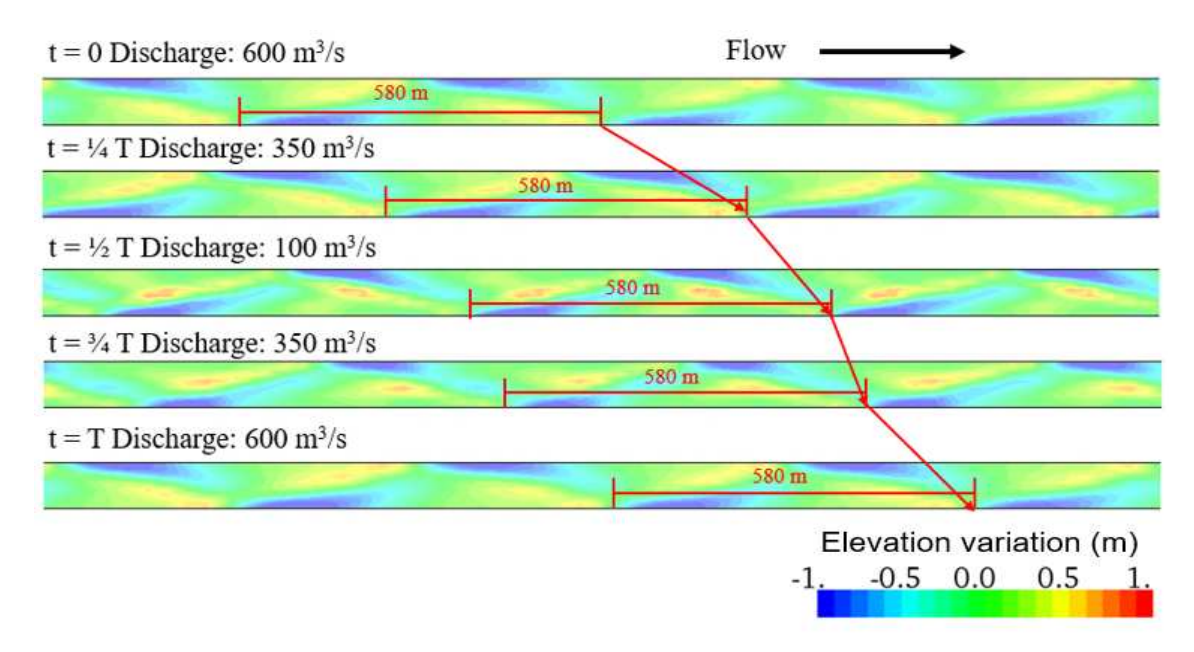


Figure 3 (Color) Alternate bars migration within one hydrograph cycle of the last hydrograph in the computation, where T is the hydrograph cycle (40 h).

To investigate the migration characteristics in greater detail, as shown in Figure 2, we selected a point at the distance axis and demonstrated the elevation variation with the time as shown in Figure 4(a). The space between two adjacent minimum values represents the time taken by an alternate bar needs to pass through this point. To simplify this description, we define this time as the "migration period". Similarly, if we select a point on the time axis, we can obtain elevation variation at the right bank for this time point in Figure 4 (b). The space between two adjacent minimum values represents the wavelength of an alternate bar.

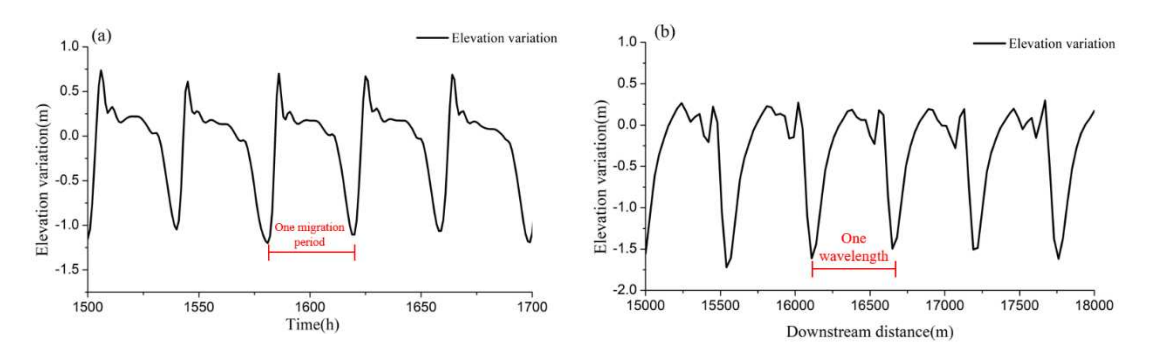


Figure 4 (a) Elevation variation with time for one point at the right bank of the river. (b) Elevation variation along the river in a downstream direction and at a single point in time.

Figure 4 shows a simple introduction of the elevation variation with respect to time and space. Figure 4 (a) shows the migration period of alternate bars, which is equal to the hydrograph cycle

of 40 h; Figure 4 (b) reflects the wavelength of alternate bars, which is a constant (580 m).

However, elevation variation at a single position or a single point in time, as shown in Figure 4, is not sufficient in obtaining the overall characteristics of simulated alternate bar dynamics. For this, we performed Fast Fourier Transform (FFT) on the bed elevation data along the right bank to obtain the temporal change of the dominant wavelength. In addition, we applied wavelet analysis for the temporal change of the bed elevation at a certain fixed point to detect the migration period of the alternate bars. Figure 5 shows the result of FFT and wavelet analysis. The results show that during the entire calculation time, the wavelength and migration period of alternate bars remain at 580 m and 40 h, respectively, suggesting consistent migration and shape characteristics of alternate bars in time and space. In addition, the migration period was equal to the hydrograph cycle. This result shows that even under an unsteady water discharge condition, the bar shape and migration pattern reach an equilibrium state in the context of long-term morphological change.

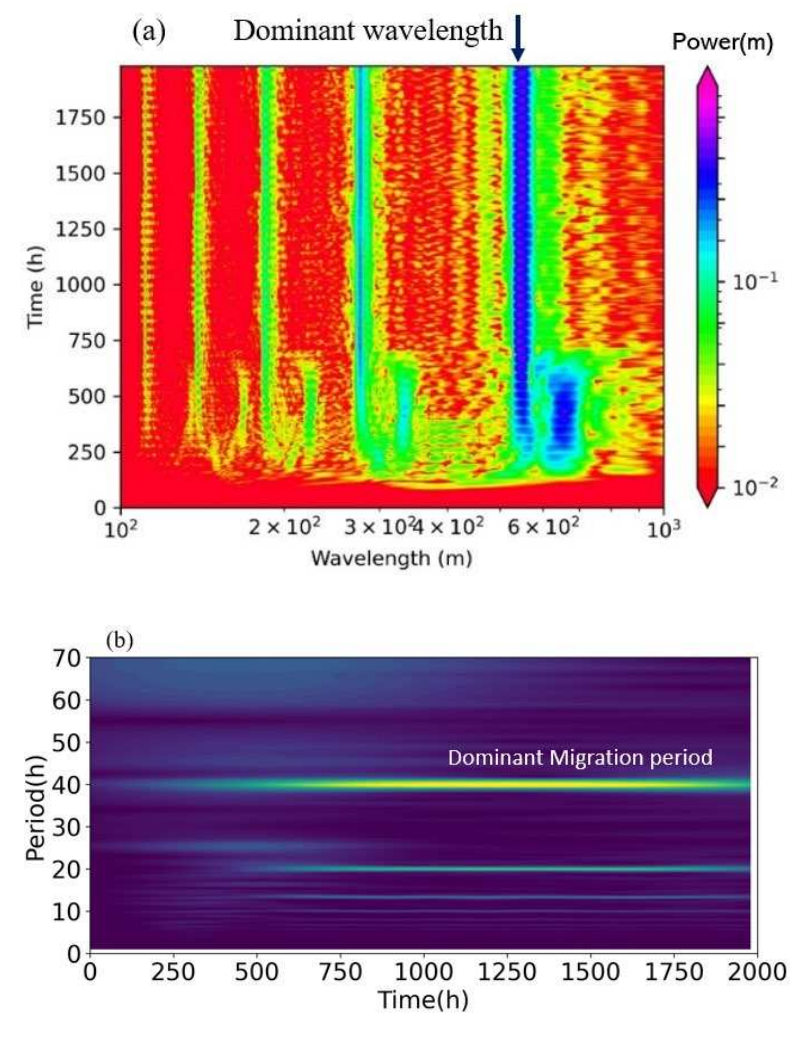


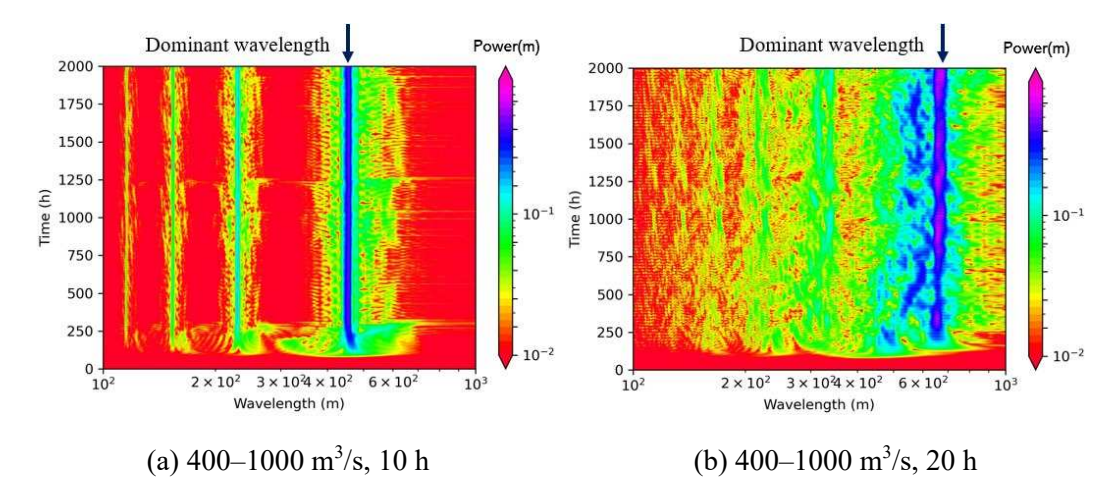
Figure 5 (a) (Color) FFT analysis of the dominant wavelength. (b) Wavelet analysis of the migration period.

3.2 The conditions and criteria for the formation of morphodynamic equilibrium state

We imposed a repeated, identical, simple triangle-shape hydrograph for this alternate bar calculation, such that properties of the hydrograph, i.e., cycle and discharge range, might control this morphodynamic equilibrium state. Alternate bars showed unconventional characteristics such as constant wavelength and migration periods after reaching morphodynamic equilibrium.

To confirm whether this phenomenon widely occurs in various unsteady flow conditions or is unique under this condition, we compare simulation results of other unsteady flow conditions by changing the minimum and maximum discharges to 400-1000 m³/s. For each case, different hydrograph cycles of 10, 20, 40 and 80 hours are tested. The reason choosing 400-1000 m³/s to study is that the lowest discharge of 400 m³/s resulted in a fully transported condition of alternate bars, while the bars remained submerged and actively moved downstream. The highest discharge of 1000 m³/s can be determined by the upper transition limit between alternate bar formation and a no-bar condition based on the linear stability analysis.

Figures 6 and 7 show the FFT and wavelet analyses of the discharge varying between 400 and 1000 m³/s, with different hydrograph cycles. These figures show that hydrograph cycles of 10 and 20 h resulted in a constant wavelength and migration period with respect to time, suggesting that in both cases, alternate bars reached morphodynamic equilibrium. The constant wavelengths for the 10 and 20 h cases were 480 m and 680 m, respectively. Meanwhile, the alternate bars with hydrograph cycles of between 40 and 80 h did not reach morphodynamics equilibrium, implying that the dominant wavelength and migration period vary with time.



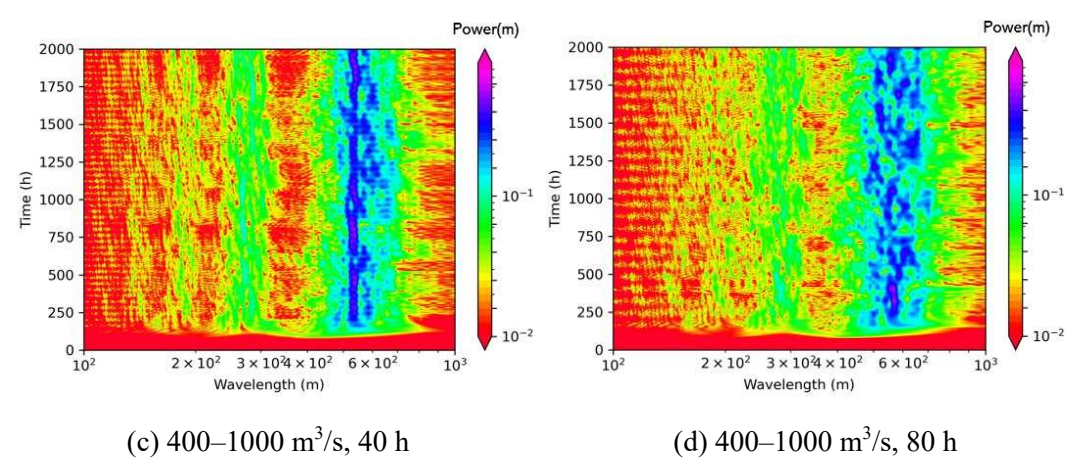


Figure 6 (a)–(d) (Color) FFT analysis of dominant wavelength in cases 400–1000 m³/s, cycles of 10, 20, 40 and 80 h.

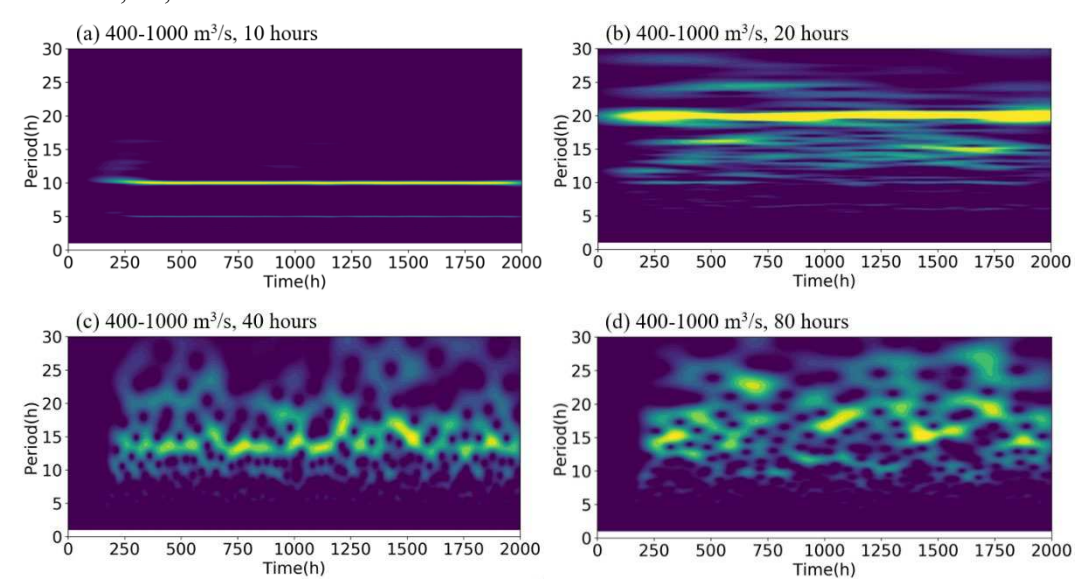


Figure 7 (Color) Wavelet analysis of the migration periods of the unsteady flow cases of 400-1000 m³/s with hydrograph cycles of (a)–(d)10, 20, 40, and 80 h.

The results of the sensitivity analysis led to the following observations: First, under fixed discharge variation (e.g., 400-1000m³/s case), morphodynamics equilibrium can be reached in different hydrograph cycle (i.e., 10 and 20 h for this case); second, hydrograph cycles determine the characteristics of alternate bars of this state, meaning that longer hydrograph cycle provides longer alternate bars.

4. Conclusions

In this study, we numerically investigated the morphodynamics of alternate bars under unsteady flow conditions. Particularly, the morphodynamics of migrating alternate bars subjected to repeated simple triangle hydrographs was simulated using a two-dimensional morphodynamic model, iRIC-Nays2DH, to understand long-term behaviors of alternate bars under unsteady discharge conditions. We found that the morphodynamics of alternate bars under a specific combination of discharge variation and hydrograph cycle reached an equilibrium state, that is, the wavelength and migration period of alternate bars remained constant, and the migration period was the same as the hydrograph cycle. This might be a unique morphodynamic feature of alternate bars under unsteady conditions because the steady discharge counterparts demonstrated a dynamic equilibrium state with slightly time-dependent features of the wavelength and migration period but did not exhibit non-time-dependent features. When morphodynamic equilibrium was reached, the hydrograph cycle was the dominant factor for alternate bar characteristics. If this morphodynamic state was achieved, the wavelength of alternate bars increased with the hydrograph cycle, and the migration period was always identical to the hydrograph cycle.

As the morphodynamic equilibrium of alternate bars under repeated unsteady discharge hydrographdiffers from a dynamic equilibrium state provided by the steady discharge analysis, the findings of this study will shed some light on the alternate bar dynamics and related channel-scale morphodynamics such as a river meandering under long-term unsteady discharge. However, the discussion in this paper is still limited because, for example, physical mechanisms of this equilibrium state and applicability of other river and hydraulic conditions remain unsolved. Further research is of immense importance in contributing to a comprehensive understanding of the long-term processes involved in migrating alternate bars under unsteady discharge conditions.

References:

M. Tubino, Growth of alternate bars in unsteady flow, J. Water Resources Research, (1991), 27(1): 37–52. https://doi.org/10.1029/90wr01699.

Y. Watanabe, M. Tubino, G. Zolezzi, et al, Behavior of alternate bars under unsteady flow conditions, C. 2nd IAHR Symposium On River, Coastal and Estuary Morphodynamics, Obihiro, Japan. Sapporo, Japan: Hokkaido Univ. Press, (2001): 673–682.

N. Izumi, M. Takatsu, S. Kawamura, Effects of the variation of discharge on the growth of fluvial bars, Journal of Japan Society of Civil Engineers, Ser. A2 (Applied Mechanics), (2021), 77(2): I_451-456. https://doi.org/10.2208/jscejam.77.2_i_451.

P. Hall, Alternating bar instabilities in unsteady channel flows over erodible beds, Journal of Fluid Mechanics, (2004), 499: 49–73. https://doi.org/10.1017/s0022112003006219.

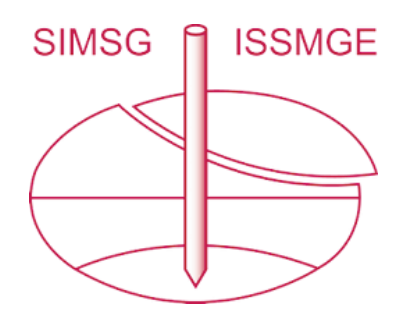
F. Visconti, C. Comporeale, L. Ridolfi, Role of discharge variability on pseudomeandering

- channel morphodynamics: Results from laboratory experiments, Journal of Geophysical Research, (2010), 115: F04042. https://doi.org/10.1029/2010jf001742.
- T. Iwasaki, Y. Shimizu, I. Kimura, Numerical simulation of bar and bank erosion in a vegetated floodplain: A case study in the Otofuke River, J. Advances in Water Resources, (2016), 93: 118–134. https://doi.org/10.1016/j.advwatres.2015.02.001.
- J.M. Nelson, Y. Shimizu, T. Abe, et al, The international river interface cooperative: Public domain flow and morphodynamics software for education and applications, J. Advances in Water Resources, (2016), 93: 62–74. https://doi.org/10.1016/j.advwatres.2015.09.017.
- T. Kang, I. Kimura, Y. Shimizu, Numerical simulation of large wood deposition patterns and responses of bed morphology in a braided river using large wood dynamics model, J. Earth Surface Processes and Landforms, (2020), 45(4): 962–977. https://doi.org/10.1002/esp.4789.
- P. Rahman, M.S. Ali, Change in transverse slope of water surface at river bend: A numerical study, J. Journal of Engineering Science, (2021), 12(2): 93–101. https://doi.org/10.3329/jes.v12i2.54634.
- A.D. Tamminga, B.C. Eaton, C.H. Hugenholtz, UAS based remote sensing of fluvial change following an extreme flood event, J. Earth Surface Processes and Landforms, (2015), 40(11): 1464 1476. https://doi.org/10.1002/esp.3728.
- H. Dai, T. Iwasaki, Y. Shimizu, Effect of sediment supply on morphodynamics of free alternate bars: Insights from hydrograph boundary layer, J. Water, (2021), 13(23): 3437. https://doi.org/10.3390/w13233437.
- L.G. MacKenzie, B.C. Eaton, Large grains matter: contrasting bed stability and morphodynamics during two nearly identical experiments, J. Earth Surface Processes and Landforms, (2017), 42(8): 1287–1295. https://doi.org/10.1002/esp.4122.
- T. Kyuka, K. Okabe, Y. Shimizu, et al, Dominating factors influencing rapid meander shift and levee breaches caused by a record-breaking flood in the Otofuke River, Japan, J. Journal of Hydroenvironment Research, (2020), 31: 76–89. https://doi.org/10.1016/j.jher.2020.05.003.
- T. Nagata, Y. Watanabe, H. Yasuda, A. Ito, Development of a meandering channel caused by the planform shape of the river bank, J. Earth Surface Dynamics, (2014), 2: 255–270. https://doi.org/10.5194/esurf-2-255-2014.
- A. Grossmann, J. Morlet, Decomposition of hardy functions into square integrable wavelets of constant shape, J. SIAM Journal on Mathematical Analysis, (1984), 15(4): 723–736. https://doi.org/10.1137/0515056.
- Y.A. Cataño-Lopera, J.D. Abad, M.H. García, Characterization of bedform morphology generated under combined flows and currents using wavelet analysis, J. Ocean Engineering, (2009), 36(9–10): 617–632. https://doi.org/10.1016/j.oceaneng.2009.01.014.
- M. Mahdade, N. Le Moine, R. Moussa, et al, Automatic identification of alternating morphological units in river channels using wavelet analysis and ridge extraction, J. Hydrology

and Earth System Sciences, (2020), 24(7): 3513-3537. https://doi.org/10.5194/hess-24-3513-2020.

M. Kuroki, T. Kishi, Regime criteria on bars and braids in alluvial straight channels, J. Proc. of JSCE, (1984), 342: 87–96. (in Japanese) https://doi.org/10.2208/jscej1969.1984.342_87.

INTERNATIONAL SOCIETY FOR SOIL MECHANICS AND GEOTECHNICAL ENGINEERING



This paper was downloaded from the Online Library of the International Society for Soil Mechanics and Geotechnical Engineering (ISSMGE). The library is available here:

https://www.issmge.org/publications/online-library

This is an open-access database that archives thousands of papers published under the Auspices of the ISSMGE and maintained by the Innovation and Development Committee of ISSMGE.

The paper was published in the proceedings of the 12th International Conference on Scour and Erosion and was edited by Shinji Sassa as the Chair of the TC213 on Scour and Erosion. The conference was held in Chongqing, China from November 4th to November 7st 2025.